International Journal of Thermophysics, Vol. 20, No. 1, 1999

Heat Capacities and Joule–Thomson Coefficients of HFC Refrigerants[1]

A. Yokozeki,[2–4] H. Sato,[2] and K. Watanabe[2]

In this report, we have examined the behavior of heat capacities and Joule–Thomson coefficients in low- and moderate-density regions based on recent theoretical studies of the ideal-gas heat capacity and virial coefficients of R-32, R-125, R-134a, R-143a, and R-152a. The results have been compared with those derived from empirical equations of state which have been recently developed, based on a large quantity of experimental data for these refrigerants. Both results are in good agreement. Proper behaviors for these second-derivative properties justify the use of the empirical equations of state in low-temperature and low-density regions where no experimental data are available.

KEY WORDS: ideal gas; heat capacity; hydrofluorocarbons; Joule–Thomson coefficient; R-32; R-125; R-134a; R-143a; R-152a; virial coefficient.

1. INTRODUCTION

Thermodynamic properties of hydrofluorocarbon (HFC) compounds have been extensively studied because of the worldwide interest in these compounds as alternative refrigerants. Many-term equations of state (EOS) such as modified BWR equations or Helmholtz functions have been proposed to correlate thermodynamic property data of HFC refrigerants, based on a large volume of experimental property data. A large quantity of data do not necessarily mean a wide range of data in PVT space. Often, data at very low and/or high temperatures are missing. Since these EOS are

[1] Paper presented at the Thirteenth Symposium on Thermophysical Properties, June 22–27, 1997, Boulder, Colorado, U.S.A.

[2] Department of System Design Engineering, Faculty of Science and Technology, Keio University, 3-14-1, Hiyoshi, Kohoku-ku, Yokohama 223, Japan.

[3] Visiting Professor from DuPont Fluoroproducts Laboratory, CRP-711, Wilmington, Delaware 19880, U.S.A.

[4] To whom correspondence should be addressed.

0195-928X/99/0100-0141$16.00/0

based on purely empirical functions of temperature, it is necessary to check the validity and the proper behavior of calculated properties in these regions. The validity range of EOS depends strongly on the proper choice of the temperature functions as well as the range of the correlated experimental data. In order to check the validity of the EOS, a critical test is to examine whether the second-derivative properties such as heat capacity (C_p or C_v) and Joule–Thomson coefficient (μ) behave properly at low temperatures, where no experimental data are available. A theoretical basis is required for this assessment. For low- and moderate-density gases, truncated virial equations of state may be used together with the ideal-gas heat capacity, $C_p^0(T)$. To illustrate, when the two-term virial equation ($Z = 1 + B(T)/V$) is valid, the heat capacities and Joule–Thomson coefficient are given by

$$C_p = C_p^0 - TP\frac{d^2B}{dT^2}, \qquad C_v = C_p^0 - R - \left(T\frac{d^2B}{dT^2} + 2\frac{dB}{dT}\right)P$$

and

$$\mu(P=0) = \left(T\frac{dB}{dT} - B\right)\Big/ C_p^0$$

respectively. Recently, we have made theoretical calculations for C_p^0 and the virial coefficients of various HFC compounds [1]. In this report, the proper behaviors of C_v, C_p, and μ for R-32, R-125, and R-143a are examined using those theoretical results.

2. IDEAL-GAS HEAT CAPACITY

The ideal-gas heat capacity, C_p^0, is obtained experimentally, e.g., from speed-of-sound data by extrapolating to the zero-pressure limit. However, the temperature range is usually narrow and limited. Theoretical values from statistical mechanical calculations are often required in order to develop EOS for a wide range of temperatures. In the past there have been significant disparities between the experimentally derived C_p^0 and the theoretical ones for various HFC compounds. Therefore, we have recently made new calculations for C_p^0 for several HFC compounds, and the results are in good agreement within about 0.2% with selected experimental values of C_p^0 in the literature [1]. For convenience, they are correlated here with the following equation:

$$C_p^0/R = \sum_n a_n(T/T_1 - T_0)^n \tag{1}$$

Table I. Coefficients in Eq. (1) for Ideal-Gas Heat Capacities[a]

	R-32	R-125	R-134a	R-143a	R-152a
a_0	6.169087	1.367753×10	1.245089×10	9.523304	1.014258×10
a_1	1.009646	1.833764	1.801270	2.100286	1.704048
a_2	-1.515960×10^{-2}	-2.225800×10^{-1}	-2.023163×10^{-1}	-1.260605×10^{-1}	-1.242065×10^{-1}
a_3	-3.221814×10^{-3}	-3.333652×10^{-3}	-7.333155×10^{-3}	-1.952249×10^{-2}	-2.195255×10^{-2}
a_4	6.740570×10^{-3}	4.226685×10^{-3}	7.263184×10^{-3}	2.288818×10^{-3}	8.522034×10^{-3}
a_5	7.319026×10^{-4}	5.010408×10^{-4}	5.424829×10^{-5}	0.0	4.943119×10^{-4}
a_6	-2.985001×10^{-4}	-1.964569×10^{-4}	-2.632141×10^{-4}	0.0	-3.929138×10^{-4}
T_0	4.0	4.1	4.1	3.1	4.1
T_1 (K)	100.0	100.0	100.0	100.0	100.0

[a] Valid range: $100\ \text{K} \leqslant T \leqslant 700\ \text{K}$.

The dimensionless coefficients and constants are given in Table I for R-32, R-125, R-134a, R-143a, and R-152a. The valid temperature range for these coefficients is from 100 to 700 K, where the original C_p^0 values [1] are reproduced within 0.1%. This temperature range is wide enough to develop comprehensive EOS for these HFC compounds.

3. VIRIAL COEFFICIENTS

HFC compounds are highly polar molecules, some of which possess higher electric dipole moments than water and ammonia. We have investigated the second (B) and third (C) virial coefficients of various HFC molecules based on the Stockmayer potential, which includes the dipole–dipole interaction of polar compounds [1]. Experimentally derived $B(T)$ and $C(T)$ coefficients have been well reproduced with physically reasonable molecular constants. Although the B and C coefficients based on the Stockmayer potential can be expressed analytically, they contain an infinite number of terms and are based on the high-temperature approximation; that is, reasonably accurate calculations are made at high temperatures relative to the potential well depth, ε/k. Particularly, at temperatures near and below the maximum in C, the numerical convergence for the C coefficients becomes extremely slow, and the calculated values have large uncertainties. In this study, we have developed analytical representations for the $B(T)$ and $C(T)$ coefficients. Weber [2] has successfully made a general correlation for the B and C coefficients of HFC compounds using semi-empirical equations. We have adopted his functional forms, and coefficients of the equations have been determined to fit our theoretical values [1] at high temperatures: 180–550 K for B and about

Table II. Coefficients of Eq. (1) for the Second Virial Coefficients[a]

	R-32	R-125	R-134a	R-143a	R-152a
b_0	1.677893×10^{-1}	1.355993×10^{-1}	1.503945×10^{-1}	1.501672×10^{-1}	1.710755×10^{-1}
b_1	-5.097407×10^{-1}	-4.445562×10^{-1}	-4.885542×10^{-1}	-4.697973×10^{-1}	-5.285915×10^{-1}
b_2	3.209336×10^{-1}	2.728313×10^{-1}	3.168288×10^{-1}	2.995867×10^{-1}	3.336846×10^{-1}
b_3	-3.619543×10^{-1}	-3.004516×10^{-1}	-3.259008×10^{-1}	-3.374173×10^{-1}	-3.378442×10^{-1}
b_4	-4.702268×10^{-3}	-3.608471×10^{-3}	-4.008385×10^{-3}	-4.579981×10^{-3}	-3.674563×10^{-3}
T_c (K)	351.4	339.4	374.5	346.3	386.4
P_c (MPa)	5.793	3.629	4.055	3.787	4.517

[a] $R = 8.314471\ \mathrm{J \cdot mol^{-1} \cdot K^{-1}}$.

330–600 K or 400–650 K for C. The functions used here are slightly modified from those of Weber:

$$\frac{BP_c}{RT_c} = a_0 + \frac{a_1}{T_r} + \frac{a_2}{T_r^2} + \frac{a_3}{T_r^3} + \frac{a_4}{T_r^8} \tag{2}$$

$$\frac{CP_c^2}{R^2T_c^2} = c_0 + \left(\frac{BP_c}{RT_c} - c_1\right)^2 \left(c_2 + \frac{c_3}{T_r^4}\right) \tag{3}$$

The dimensionless coefficients and constants are given in Tables II and III for R-32, R-125, and R-134a, R-143a, and R-152a. These coefficients reproduce the theoretical B and C within 0.1% for the temperatures used in the fit.

4. HEAT CAPACITIES AND JOULE–THOMSON COEFFICIENTS

For moderate- and low-density gases, the three-term virial equations of state may be used:

$$Z = 1 + B(T)/V + C(T)/V^2 \tag{4}$$

Table III. Coefficients of Eq. (3) for the Third Virial Coefficients

	R-32	R-125	R-134a	R-143a	R-152a
c_0	9.662228×10^{-10}	1.764620×10^{-9}	1.976592×10^{-9}	1.582560×10^{-9}	3.603253×10^{-9}
c_1	1.302729×10^{-1}	8.591696×10^{-2}	8.737402×10^{-2}	1.054123×10^{-1}	9.046746×10^{-2}
c_2	3.671696×10^{-7}	3.161471×10^{-7}	3.270633×10^{-7}	3.649605×10^{-7}	3.661666×10^{-7}
c_3	-9.073470×10^{-8}	-1.068222×10^{-7}	-1.107513×10^{-7}	-1.027143×10^{-7}	-1.058910×10^{-7}

Then isochoric, C_v, and isobaric, C_p, heat capacities are given by

$$C_v = C_p^0 - R - RT\left(T\frac{d^2B}{dT^2} + 2\frac{dB}{dT}\right)\Big/V - \frac{R}{2}\left(\frac{T}{V}\right)^2\left(\frac{d^2C}{dT^2} + \frac{2}{T}\frac{dC}{dT}\right) \quad (5)$$

$$C_p = C_v + R\left[1 + \left(T\frac{dB}{dT} + B\right)\Big/V + \left(T\frac{dC}{dT} + C\right)\Big/V^2\right]^2\Big/\left(1 + \frac{2B}{V} + \frac{3C}{V^2}\right) \quad (6)$$

C_v and C_p along isobars have been calculated as a function of temperature for all compounds in the present study, and some examples are shown inlets. Figs. 1–4 for R-32, R-125, and R-143a compared with those calculated from recently developed empirical EOS [3–5]. In the case of R-32, the pronounced negative slope, $(\partial C_v/\partial T)_p$, near the saturation boundary is striking at low pressures, while R-125 has a positive slope at the corresponding pressures. Similar behaviors are seen for C_p. It has been found that the behavior of the negative or positive slope is related to the magnitude of the slope of the second virial coefficient. All EOS examined in the present study show theoretically correct behaviors as seen in the figures. While the absolute agreement is good, however, near the saturation boundary the curves from the current work seem to have slightly but systematically less curvature than those from the EOS, particularly at high pressures. This is due mainly to the fact that the simple three-term virial equation of state used in this work becomes less accurate in the high-density regions.

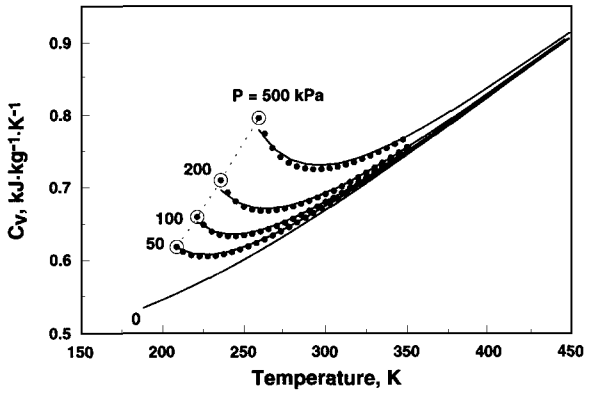

Fig. 1. Vapor phase C_v [$kJ \cdot kg^{-1} \cdot K^{-1}$] of R-32 at constant pressure as a function of temperature. (—) Theory; (○) saturation boundary, (●) Ref. 3.

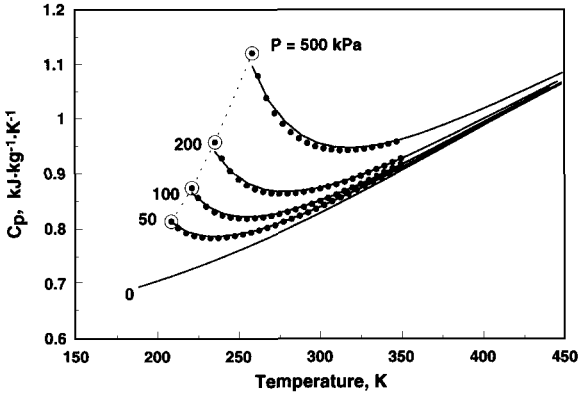

Fig. 2. Vapor phase C_p [kJ · kg^{-1} · K^{-1}] of R-32 at constant pressure as a function of temperature. (—) Theory; (○) saturation boundary, (●) Ref. 3.

The Joule–Thomson coefficient, μ, and the zero-pressure coefficient, $\mu(0)$, are;

$$\mu \equiv \left(\frac{\partial T}{\partial P}\right)_H = \frac{1}{C_p}\left[T\frac{dB}{dT} - B + \left(T\frac{dC}{dT} - 2C\right)\Big/V\right]\Big/\left(2Z - 1 + \frac{C}{V^2}\right) \tag{7}$$

$$\mu(0) = \frac{1}{C_p^0}\left(T\frac{dB}{dT} - B\right) \tag{8}$$

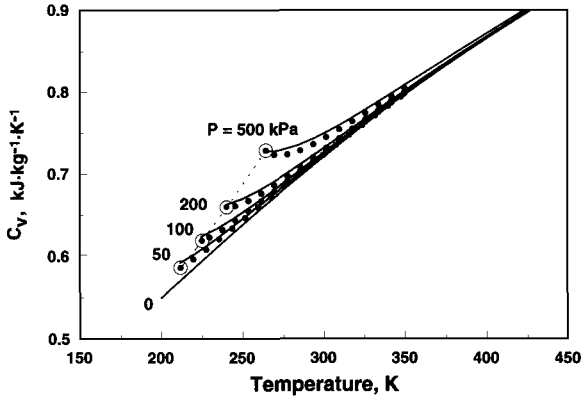

Fig. 3. Vapor phase C_v [kJ · kg^{-1} · K^{-1}] of R-125 at constant pressure as a function of temperature. (—) Theory; (○) saturation boundary, (●) Ref. 4.

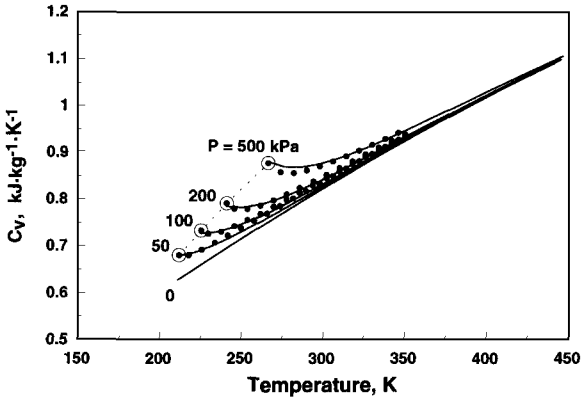

Fig. 4. Vapor phase C_v [kJ · kg^{-1} · K^{-1}] of R-143a at constant pressure as a function of temperature. (—) Theory; (○) saturation boundary, (●) Ref. 5.

The difference, $\mu(P) - \mu(0)$, at constant pressures has been calculated as a function of temperature for all compounds in the present study, and some examples are shown in Fig. 5 for R-32 and in Fig. 6 for R-125. The results for these two refrigerants are qualitatively different; the difference for R-32 is negative near the saturation boundary, while that for R-125 is positive. For other HFC compounds, R-134a, R-143a, and R-152a, the results are similar to the case of R-125. These behaviors have been explained by the

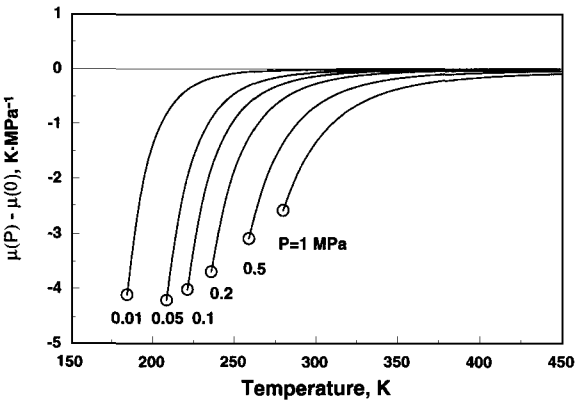

Fig. 5. Differences in Joule–Thomson coefficients, $\mu(P) - \mu(0)$ [K · MPa^{-1}], of R-32 at constant pressure as a function of temperature. (—) Theory; (○) saturation point.

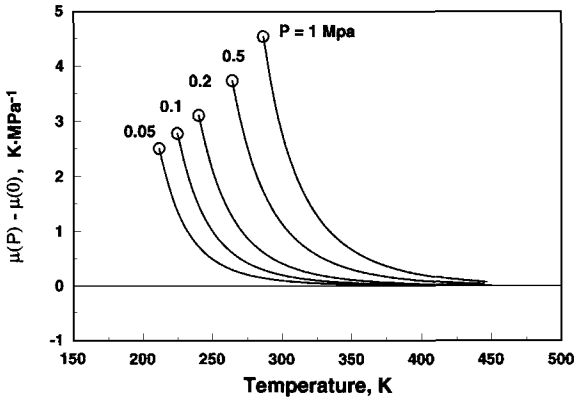

Fig. 6. Differences in Joule–Thomson coefficients, $\mu(P) - \mu(0)$ [$K \cdot MPa^{-1}$], of R-125 at constant pressure as a function of temperature. (—) Theory; (○) saturation point.

relative magnitude of C_p^0, as well as the magnitudes of the virial coefficients. More general and theoretical behaviors for heat capacities and Joule–Thomson coefficients, including high-pressure fluids and low-temperature liquids, will be studied in the future.

5. CONCLUSION

For low- and moderate-density gases of R-32, R-125, R-134a, R-143a, and R152a, the behaviors of heat capacities and Joule–Thomson coefficients are theoretically investigated based on our recent calculations of ideal-gas heat capacities and virial coefficients. The empirically developed equations of state examined in this study are found to be both qualitatively and quantitatively consistent with existing theoretical results.

ACKNOWLEDGMENT

The authors thank the New Energy and Industrial Technology Development Organization, Tokyo for financial support of the present study.

REFERENCES

1. A. Yokozeki, H. Sato, and K. Watanabe, *Int. J. Thermophys.* **19**:89 (1998).
2. L. A. Weber, *Int. J. Thermophys.* **15**:461 (1994).
3. R. Tillner-Roth and A. Yokozeki, *J. Phys. Chem. Ref. Data* **26**:1273 (1998).
4. H. Sunaga, R. Tillner-Roth, H. Sato, and K. Watanabe, *Int. J. Thermophys.* (in press).
5. J. Li, R. Tillner-Roth, H. Sato, and K. Watanabe, *Int. J. Thermophys.* (in press).